JOURNAL OF THE KOREAN ASTRONOMICAL SOCIETY
34: S337 ~ S339, 2001

Numerical Simulation of a Protostar Flare Loop between the Core and Disk

HIROAKI ISOBE [1], TAKAAKI YOKOYAMA [2], AND KAZUNARI SHIBATA [1]
[1] Kwasan and Hida Observatories, Kyoto University, Kyoto 607-8471, Japan
[2] Nobeyama Radio Observatory, National Astronomical Observatory, Minamisaku, Nagano 384-1305, Japan
(Received Oct. 1, 2001; Accepted Nov. 15, 2001)

ABSTRACT

One-dimensional hydrodynamic modeling of a protostellar flare loop is presented. The model consists of thermally isolated loop connecting the central core and the accretion disk. We found that the conductive heat flux of a flare heated the accretion disk up to coronal temperature and consequently the disk is evaporated and disappeard. This effect may explain the ovserved feature of the repeated flare from the young stellar object YLW 15.

Key Words : methods: numerical — hydrodynamics — stars: flare

I. Introduction

Recently Tsuboi et al. (2000) observed three X-ray flares from the young stellar object (YSO) YLW 15 with ASCA. The flares occurred every ~ 20 hr repeatedly. Figure 1 shows the time profiles of the X-ray intensity (top panel), the plasma temperature (middle panel) and the emission measure (bottom panel). The plasma temperature shows a fast rise and slow decay for each flare, while the emission measure (EM) shows this time profile only for the first flare, and remains almost constant during the second and third flares. Solar flares which occur in the same location repeatedly are called homologous flares, and each flare usually shows a clear rise and decay in emission measure profile. So the observed behavior of the emission measure profiles of the repeating protostar flares is quite different from that of typical solar flares.

In solar flares, the magnetic energy in the corona is converted into the thermal energy of hot ($\sim 10^7$ k) plasma via magnetic reconnection. The released energy heats the cool ($\sim 10^4$ K) plasma in the chromosphere mainly by conduction, and the heated chromospheric plasma is evaporated into the corona and fills the closed flare loop. This process increases the emission measure. On the other hand, protostellar flares are considered to occur in long loops connecting the central core and the accretion disk (e.g., Hayashi, Shibata, & Matsumoto 1996). The main differences from solar flares are the size ($\sim 10^{11-12}$ cm; one or two order of magnitude longer than that of solar flares) and the accretion disk. The longer flare loop causes smaller gravity and smaller conductive loss rate. Evaporation from the accretion disk may cause different behavior of the time profile of the emission measure.

To investigate the evolution of a flare loop in the circumstance of a protostar, we have performed hydrodynamical simulation including the thermal conduction. In particular we have examined the evaporation from the accretion disk and its effect on the emission measure profile.

II. Numerical Model

Figure 2 shows a schematic picture of the model of a protosteller flare loop. We calculate the dynamics of magnetically confined plasma in the flare loop using one-dimensional hydrodynamic code. The loop penetrates the accretion disk with both ends anchored in the photoshere of the central core. The length of the loop is 3.6×10^7 km and the geometry is assumed to be semi-circular with constant cross section. The mass and radius of the central star are set to be $1M_\odot$ and $4R_\odot$ respectively. The gravity of the accretion disk and the effect of rotation are not taken into account. The heat deposition of flare takes place at the middle portion between the star and the disk. The loop is initially in hydrostatic equilibrium, but not in strict energy equilibrium. The heating function $H(s,t)$ is given by $H(s,t) = H_q(s) + H_f(s,t)$, where s is the distance along the loop from its base, and t is the time. The first term $H_q(s)$ is assumed to balance radiative losses in the initial condition at each point. The radiative loss function is chosen to approximate the form for a plasma with normal solar abundances. The thermal conductivity is taken to be of the classical Spitzer form (Spitzer 1962) and the resulting heat flow is assumed not to be flux-limited. The flare heating function is of the form of spatially Gaussian and a step function in time; $H_f(s,t) = E(t)\exp[-(s-s_{flr})^2/2\sigma^2]$, where E(t) is the total heat flux for a loop, which is maintained for about 0.9 hour. s_{flr} and σ are set to be 4.5×10^{11} cm and 9.6×10^9 cm respectively. Hori et al. (1997) used basically the same code for a numerical modering of solar flare loops. Numerical algorithm is described in the Appendix of Hori et al. (1997) in detail.

III. Results and Discussion

We present the results of two heating cases. In both cases flare heating occur twice at $t = 0$ and $8(hr)$. Only the total heat flux E is different between the two cases. Other parameters such as loop length or flare duration are fixed.

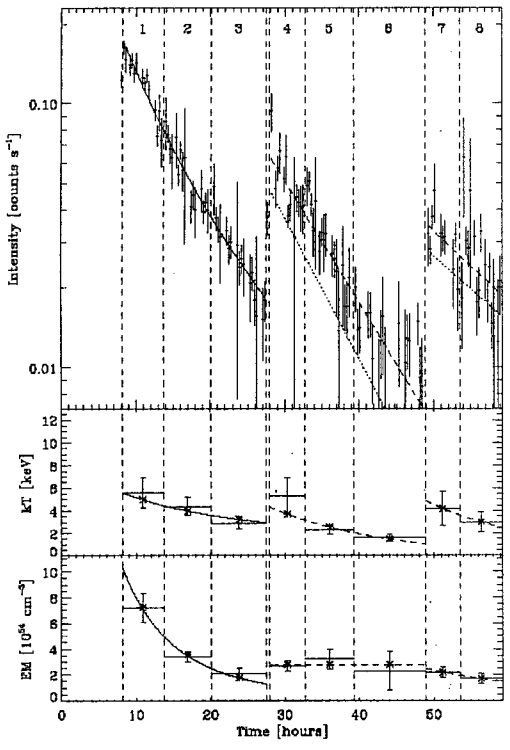

Fig. 1.— Light curve (top), temperature (middle), and emission measure (bottom) of the quasi-periodic X-ray flares from YLW 15. (Figure 2 of Tsuboi et al. (2000))

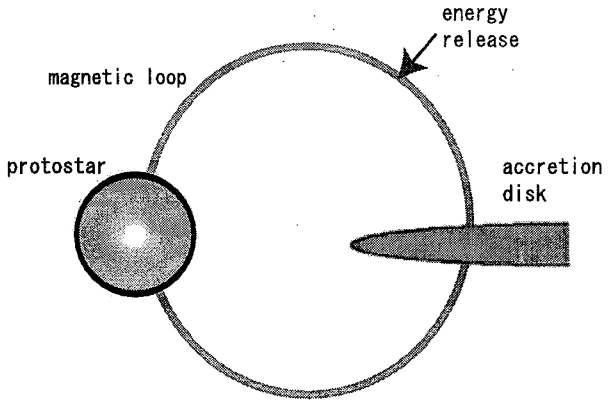

Fig. 2.— Schematic picture of a protostellar flare loop connecting the core and the accretion disk.

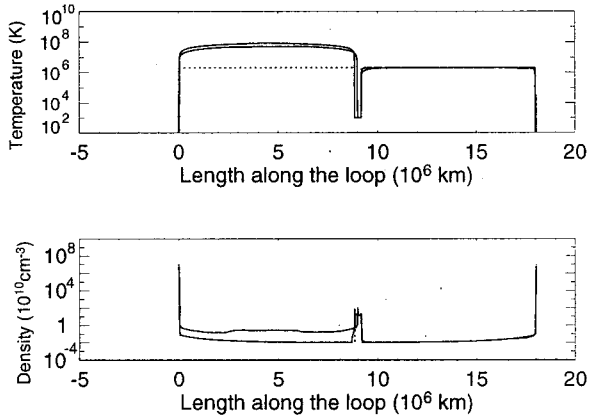

Fig. 3.— Temperature and density distribution of *Case A*. The plotting times are $t = 0.077$ and 2.24 hr. The dashed lines show the initial values.

Case A: $E = 1.6 \times 10^9/(\sigma\sqrt{\pi})$ (ergs cm^{-2} s^{-1}) for the first flare and $E = 8 \times 10^8/(\sigma\sqrt{\pi})$ (ergs cm^{-2} s^{-1}) for the second flare. Figure 3 shows the temperature (upper panel) and density (lower panel) distribution at $t = 0.077$ and 2.24 hr. The dashed lines show the initial values. The heat conduction front impinges on the chromoshere and the accretion disk, where plasmas are rapidly heated to coronal temperatures. The resultant high pressure causes evaporation of the plasma both in the chromoshere and the disk. The flare loop between the core and the disk is filled with hot and dense plasma, whereas the other side of the loop (i.e. beyond the disk) is not affected by the flare. The propagation of the conduction front in the accretion disk and resultant evaporation of the disk plasma are shown in figure 4. The conduction front is stopped in the disk even after the second flare. The time profiles of the temperature at $s = s_{flr}$ and the emission measure of the hot (> 5 MK) plasma in the whole flare loop are shown in figure 7 (upper panel). The values of the emission measure shown by the right vertical axis are calculated assuming the aspect ratio (ratio of diameter and length of the loop) a of 0.1. Note that the emission measure increases greatly soon after the second flare ($t = 8$), due to the evaporation from both the core and the disk.

Case B: $E = 1.6 \times 10^{10}/(\sigma\sqrt{\pi})$ (ergs cm^{-2} s^{-1}) for the first flare and $E = 1.5 \times 10^9/(\sigma\sqrt{\pi})$ (ergs cm^{-2} s^{-1}) for the second flare. Figure 5 and 6 show the temperature and emission measure distribution. The remarkable feature is that the conduction front penetrates the disk and reaches at the other end (chromoshere) of the loop during the first flare. As a consequence all the plasma in the disk becomes flare temperature and spreads over the loop, i.e., the accretion disk disappears. The temperature and emission measure profiles are shown in figure 7 (lower panel). The increase in the emission measure at the second flare is relatively small compared with *case A*. This is because the accretion disk, which is a source of the evaporation plasma, disappears at the first flare and consequently effective loop length becomes longer, resulting in small conductive heat flux.

Our numerical result suggests that the evaporation and resultant disappearance of the accretion disk may explain the temperature and emission measure profiles of the repeating flares of YLW15. More parameter survey and detailed comparison with observations are important future work.

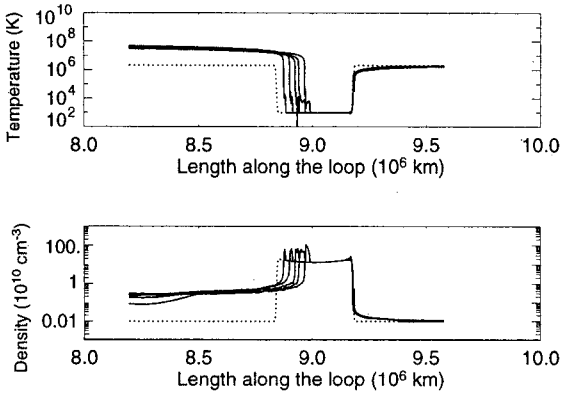

Fig. 4.— Temperature and density distribution in the accretion disk of *Case A*. The plotting time interval is 1390 sec. The dashed lines show the initial values.

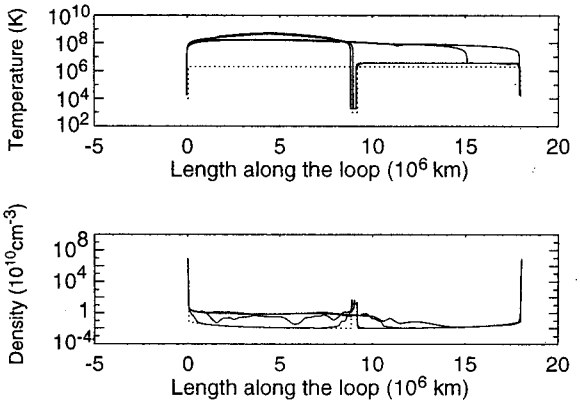

Fig. 5.— Temperature and density distribution of *Case B*. The plotting times are $t = 0.077$, 0.77, 2.24, and 2.55 hr. The dashed lines show the initial values.

REFERENCES

Favata, F., Micela, G., & Reale, F. 2001, A&A, 375, 485

Hayashi, M. R., Shibata, K., & Matsumoto, R. 1996, ApJ, 468, L37

Hori, K., Yokoyama, T., Kosugi, T., & Shibata, K. 1997, ApJ, 489, 426

Spitzer, L. 1962, Physics of Fully Ionized Gases (2d rev. ed.; New York: Interscience)

Tsuboi, Y., Imanishi, K., Koyama, K., Grosso, N., & Montmerle, T. 2000, ApJ, 532, 1089

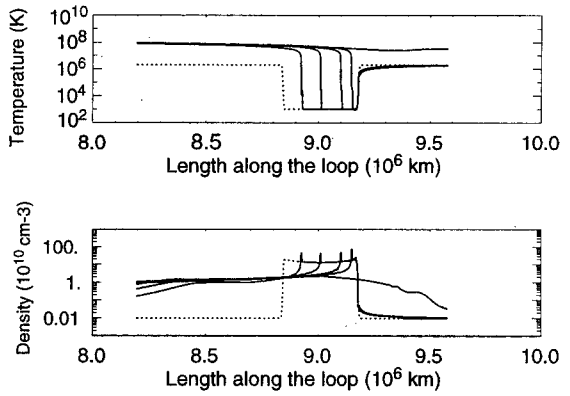

Fig. 6.— Temperature and density distribution in the accretion disk of *Case A*. The plotting time interval is 1390 sec. The dashed lines show the initial values.

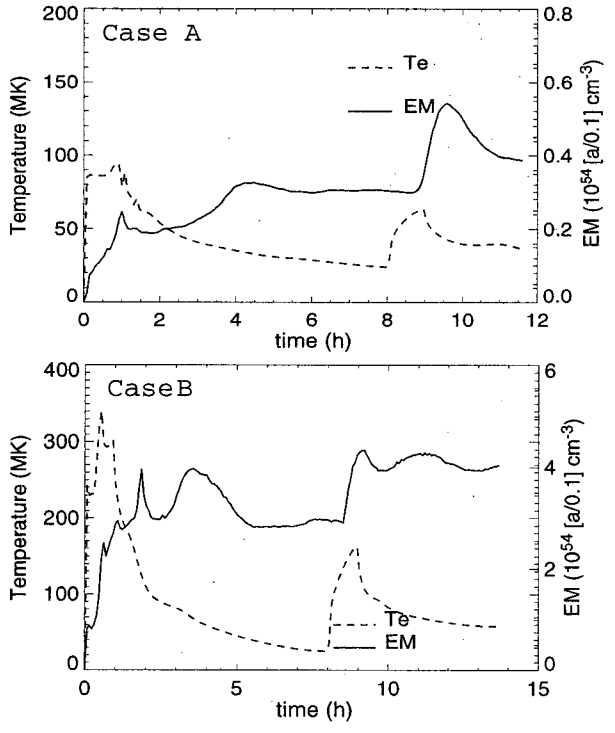

Fig. 7.— Temperature and emission measure profiles of *Case A* (upper panel) and *Case B* (lower panel). The flares occurred at $t = 0$ and 8 (hr). The right vertical axes show the emission masure calculated assuming an aspect ratio a of 0.1.